Effect of the multi-phase character of the ISM
on the dynamo in the Milky Way and other spiral galaxies

Oliver Gressel*
The Niels Bohr Institute, Copenhagen

Axel Brandenburg
— Nordita, Stockholm —

Abhijit Bendre, Detlef Elstner,
Udo Ziegler & Günther Rüdiger
— Leibniz Institute (AIP), Potsdam —

May 7 – June 2, 2017

Nordita program on Phase Transitions in Astrophysics

The Niels Bohr International Academy

* oliver.gressel@nbi.dk

contents

contents

contents

observations

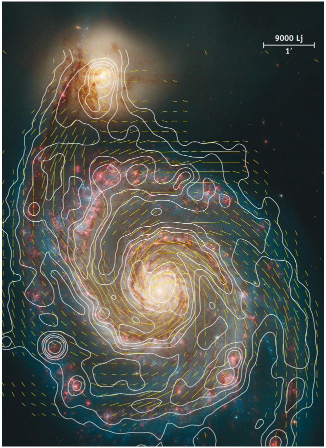

Andrew Fletcher/Rainer Beck,
SuW and Hubble Heritage Team, STScI/AURA

- What is the origin of regular galactic magnetic fields?
  - primoridial field, (i.e. frozen-in fossil record of galaxy formation)
  - dynamo-generated field, (i.e. dynamically replenished)
- Beck of the envelope
  - galactic rotation winds-up B_ϕ
    $\tau_\Omega \simeq 2\pi/25\,\mathrm{kpc}^{-1}\,\mathrm{km\,s}^{-1} \simeq 250\,\mathrm{Myr}$
  - turbulent diffusion
    $\tau_\mathrm{d} \simeq (0.5\,\mathrm{kpc})^2/0.5\,\mathrm{kpc\,km\,s}^{-1} \simeq 500\,\mathrm{Myr}$
  - large observed pitch angle strongly favours dynamo

observations

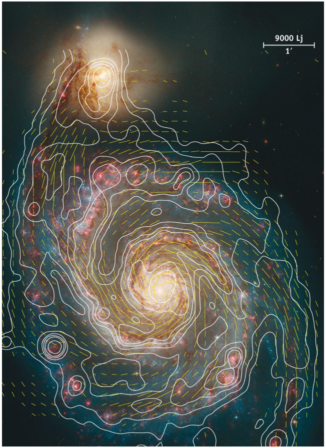

Andrew Fletcher/Rainer Beck,
SuW and Hubble Heritage Team, STScI/AURA

- What is the origin of regular galactic magnetic fields?
  - primoridial field, (i.e. frozen-in fossil record of galaxy formation)
  - dynamo-generated field, (i.e. dynamically replenished)
- Beck of the envelope
  - galactic rotation winds-up B_ϕ
    $\tau_\Omega \simeq 2\pi/25\,\mathrm{kpc}^{-1}\,\mathrm{km\,s}^{-1} \simeq 250\,\mathrm{Myr}$
  - turbulent diffusion
    $\tau_\mathrm{d} \simeq (0.5\,\mathrm{kpc})^2/0.5\,\mathrm{kpc\,km\,s}^{-1} \simeq 500\,\mathrm{Myr}$
  - large observed pitch angle strongly favours dynamo

supernova-driven turbulence

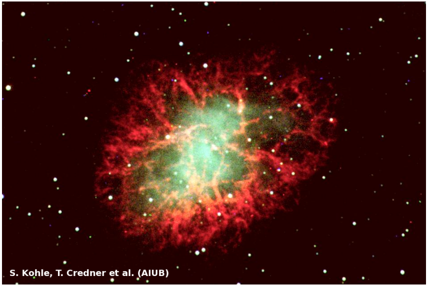

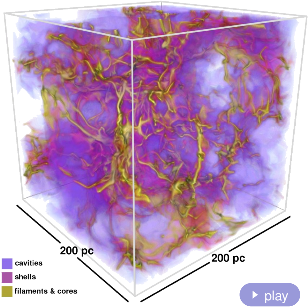

play

- small-scale dynamo is simple (stretch–twist–fold . . .)
- but how amplify regular fields in a turbulent environment?
  rotation + stratification $\rightarrow$ mean-field dynamo

the α effect dynamo

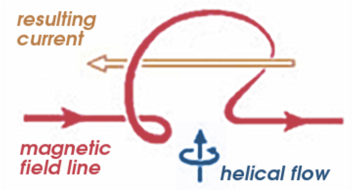

- helical α effect in a single expanding SNR ▸ play
- remnants expanding out of the galactic plane ▸ play
- breaking the homogeneity of the turbulence ▸ play

- Key mechanisms
  - rotation (and/or shear) $\rightarrow$ field-line stretching
  - helical flow component $\rightarrow$ avoid cancellation due to anti-parallel field
  - α effect couples the poloidal and toroidal field components
  - reconnection $\rightarrow$ restore original field-line topology

the big picture

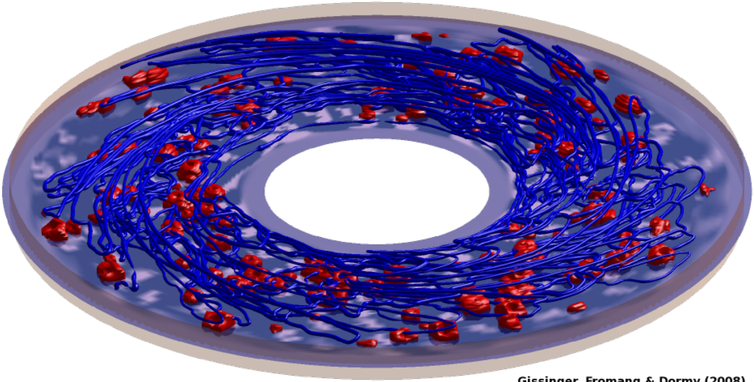

Gissinger, Fromang & Dormy (2008)

- encapsulate the effect of the supernovae
- model the evolution of the large-scale field

modelling the dynamo process

- Mean-field approach:
  - split into mean + fluctuation

    $\mathbf{U} = \overline{\mathbf{U}} + \mathbf{u}$ and $\mathbf{B} = \overline{\mathbf{B}} + \mathbf{b}$
  - derive mean-field equation

    $$\partial_t \overline{\mathbf{B}} = \nabla\times\left(\overline{\mathbf{U}}\times\overline{\mathbf{B}} + \bar{\mathcal{E}} - \eta\,\nabla\times\overline{\mathbf{B}}\right)$$

    turbulent EMF $\bar{\mathcal{E}} = \overline{\mathbf{u}\times\mathbf{b}}$

- Parametrise small-scale effects $\bar{\mathcal{E}}$ as a functional of $\overline{\mathbf{U}}$, $\overline{\mathbf{B}}$, $\overline{f(\mathbf{u})}$
  - for sufficient scale separation

    $$\bar{\mathcal{E}}_i = \alpha_{ij}\bar{B}_j - \tilde{\eta}_{ij}\,\varepsilon_{jkl}\partial_k\bar{B}_l$$

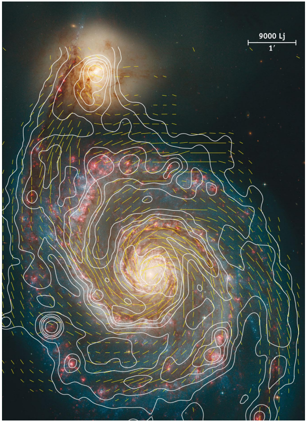

Andrew Fletcher/Rainer Beck,
SuW / Hubble Heritage Team, STScI/AURA

modelling the dynamo process

- Mean-field approach:
  - split into mean + fluctuation

    $\mathbf{U} = \overline{\mathbf{U}} + \mathbf{u}$ and $\mathbf{B} = \overline{\mathbf{B}} + \mathbf{b}$
  - derive mean-field equation

$$\partial_t \overline{\mathbf{B}} = \nabla \times \left(\overline{\mathbf{U}} \times \overline{\mathbf{B}} + \bar{\mathcal{E}} - \eta \, \nabla \times \overline{\mathbf{B}} \right)$$

turbulent EMF $\bar{\mathcal{E}} = \overline{\mathbf{u} \times \mathbf{b}}$

- Parametrise small-scale effects $\bar{\mathcal{E}}$ as a functional of $\overline{\mathbf{U}}$, $\overline{\mathbf{B}}$, $\overline{f(\mathbf{u})}$
  - for sufficient scale separation

$$\bar{\mathcal{E}}_i = \alpha_{ij} \bar{B}_j - \tilde{\eta}_{ij} \, \varepsilon_{jkl} \partial_k \bar{B}_l$$

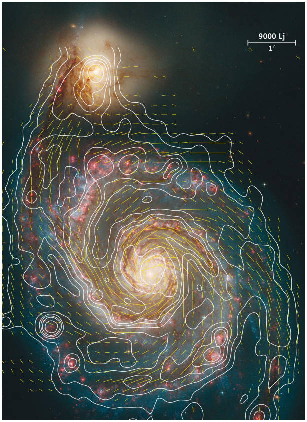

Andrew Fletcher/Rainer Beck,
SuW / Hubble Heritage Team, STScI/AURA

local box simulations

- Model geometry:
  - local patch of interstellar medium, up to 1.6 kpc on edge ($\Delta \simeq 10$ pc)
  - vertical stratification up to ± 6 kpc
  - sheared galactic rotation
- Physical ingredients:
  - non-ideal MHD (+ heat conduction)
  - optically thin radiative heating/cooling
  - localised thermal energy input modelling the supernovae

play

Korpi, Brandenburg, Shukurov, Tuominen & Nordlund (1999)

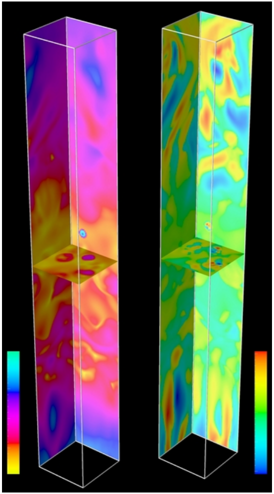

local box simulations

- Model geometry:
  - local patch of interstellar medium, up to 1.6 kpc on edge ($\Delta \simeq 10$ pc)
  - vertical stratification up to ± 6 kpc
  - sheared galactic rotation
- Physical ingredients:
  - non-ideal MHD (+ heat conduction)
  - optically thin radiative heating/cooling
  - localised thermal energy input modelling the supernovae

play

Korpi, Brandenburg, Shukurov, Tuominen & Nordlund (1999)

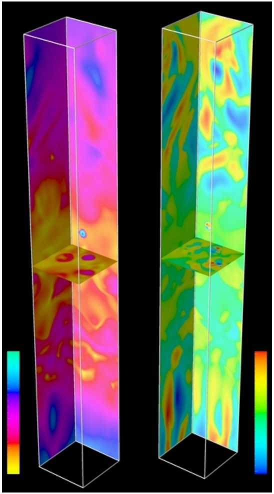

α-profiles

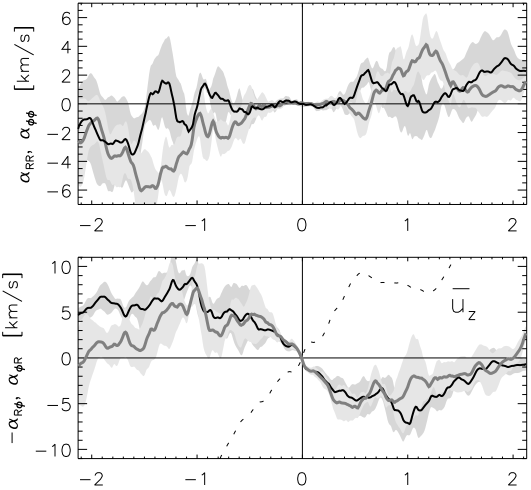

Gressel, Elstner, Ziegler & Rüdiger (2008), A&A 486, L35

- dynamo effect $|\alpha_R|,\ |\alpha_\phi| \simeq 3\,\mathrm{km\,s^{-1}}$
- diamagn. pumping $|\gamma_z| \simeq 7\,\mathrm{km\,s^{-1}}$ directed inward
- $|\alpha| : |\gamma|$ consistent w/ SOCA results
- effect of galactic wind $\bar{u}_z$ balanced by turb. pumping

$\tilde{\eta}$-profiles

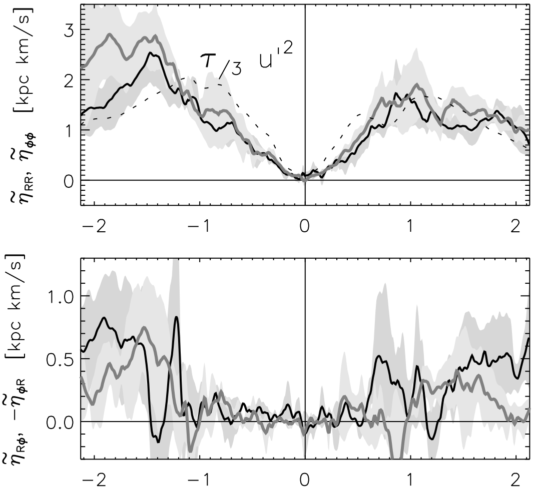

- turb. diffusivity $\simeq 2\,\mathrm{kpc\,km\,s^{-1}}$
- coherence time $\tau \simeq 3\,\mathrm{Myr}$

- non-vanishing $\Omega \times J$ effect $\delta_z \simeq 0.5\,\mathrm{kpc\,km\,s^{-1}}$
- add shear $\to$ dynamo

it really works!

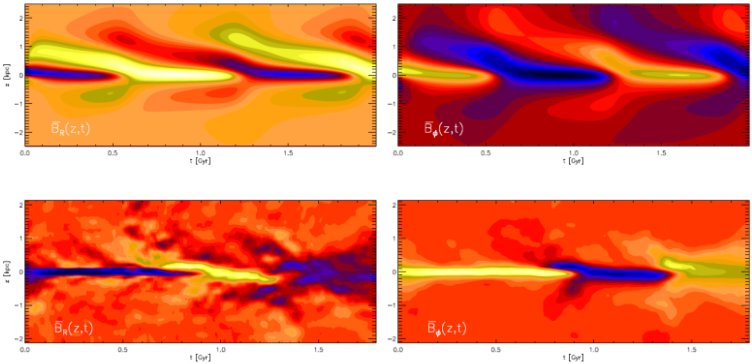

Figure 4.10: Same as Fig. 4.9, but additionally including a mixed (anti-)symmetric contribution in the off-diagonal elements of $\tilde{\eta}$ (upper panels). Now the lopsided dipolar symmetry in the field reversals persists and closely resembles the features seen in the *direct* simulation H4 (lower panels).

the role of the multi-phase flow

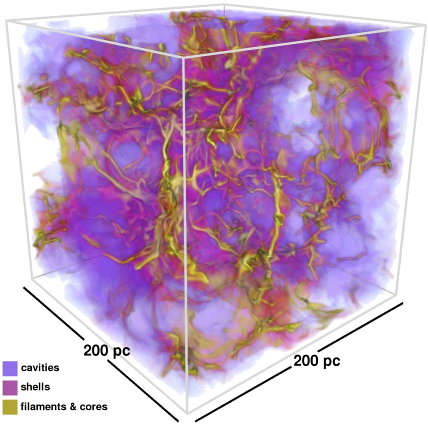

TI–MRI play play TI–SNe play

the role of the multi-phase flow

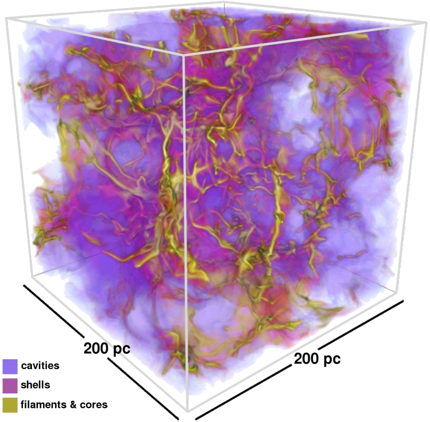

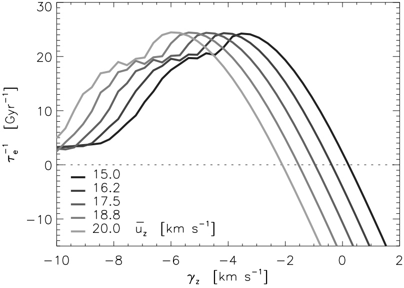

TI–MRI play play TI–SNe play

the role of the multi-phase flow

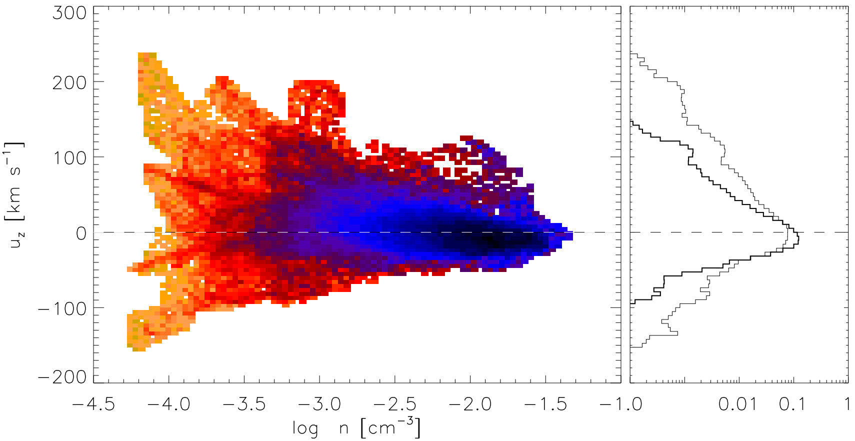

TI–MRI play play TI–SNe play

scaling relations (brute force)

- dynamo effect as function of
  - supernova rate $\hat{\sigma} = \sigma/\sigma_0$
  - rotation frequency $\hat{\Omega} = \Omega/\Omega_0$
  - midplane density $\hat{\rho} = \rho/\rho_0$

- scaling relations:

$$\alpha = 2\ \mathrm{km\,s^{-1}}\quad \hat{\sigma}^{0.4}\ \hat{\Omega}^{0.5}\ \hat{\rho}^{-0.1}$$
$$\gamma_z = 12\ \mathrm{km\,s^{-1}}\quad \hat{\sigma}^{0.5}\ \hat{\Omega}^{-0.2}\ \hat{\rho}^{0.3}$$
$$\eta = 2\ \mathrm{kpc\,km\,s^{-1}}\ \hat{\sigma}^{0.4}\ \hat{\Omega}^{0.25}\ \hat{\rho}^{0.4}$$

where $\sigma_0 = 30\mathrm{Myr}^{-1}\mathrm{kpc}^{-2}$,
$\Omega_0 = 25\mathrm{Gyr}^{-1}$, $\rho_0 = 1\,\mathrm{cm}^{-3}$

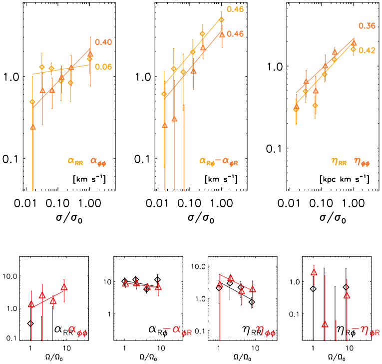

magnetic field saturation

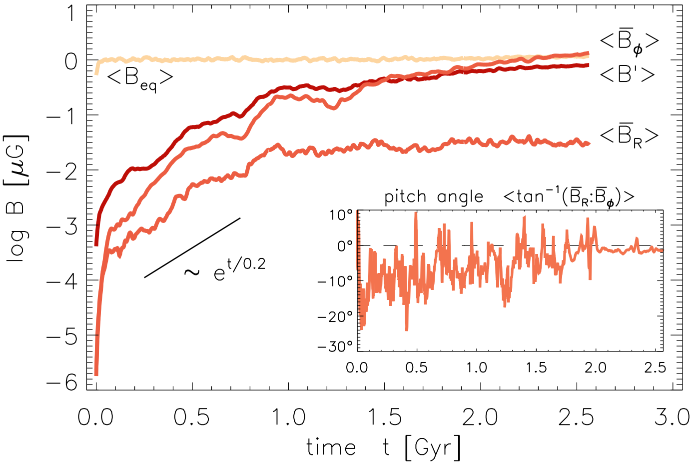

beyond the kinematic phase

- Dynamical quenching (new notation: $a = A'$, $b = B'$, $\ldots$)
  - non-linear effects in the EMF

$$\partial_t \bar{\mathcal{E}} = \overline{u \times (\partial_t b)} + \overline{(\partial_t u) \times b}$$

$$\rightarrow \qquad \alpha = \alpha_{\rm K} + \alpha_{\rm M} = -\tfrac{1}{3}\tau_{\rm K}\,\langle \omega \cdot u \rangle + \tfrac{1}{3}\tau_{\rm M}\,\langle j \cdot b \rangle \,/\rho$$

  - magnetic helicity evolution

$$\partial_t \langle \bar{A} \cdot \bar{B} \rangle = +2\,\langle \bar{\mathcal{E}} \cdot \bar{B} \rangle - 2\eta\,\langle \bar{J} \cdot \bar{B} \rangle$$

$$\partial_t \langle a \cdot b \rangle = -2\,\langle \bar{\mathcal{E}} \cdot \bar{B} \rangle - 2\eta\,\langle j \cdot b \rangle$$

  - time evolution for effective α effect

$$\partial_t \alpha \;=\; -2\eta_{\rm t}\, k_{\rm f}^2 \left(\frac{\alpha\langle \bar{B}^2\rangle \;-\; \eta_{\rm t}\langle \bar{J}\cdot\bar{B}\rangle \;+\; \text{fluxes}}{B_{\rm eq}^2} + \frac{\alpha - \alpha_{\rm K}}{\eta_t/\eta} \right)$$

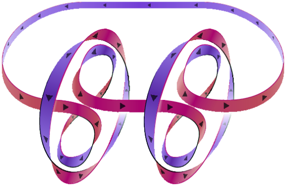

Blackman (2014)

using $\alpha_{\rm K} = \text{const.}$, $\langle \bar{\mathcal{E}} \cdot \bar{B} \rangle = \langle \alpha \bar{B} \cdot \bar{B} \rangle - \langle \eta_{\rm t} \bar{J} \cdot \bar{B} \rangle$ and $\langle a \cdot b \rangle \simeq k_{\rm f}^{-2} \langle j \cdot b \rangle$

- Blackman & Field (2000) ▪ Vishniac & Cho (2001) ▪ Blackman & Brandenburg (2002) ▪ Vishniac & Shapovalov (2014) ▪ Squire & Bhattacharjee (2015a/b)

quenching scenarios

- Stationary-state, dynamical quenching
  - general form $(\mathrm{d}\alpha/\mathrm{d}t = 0)$:

$$\alpha \;=\; \frac{\alpha_{\rm K} \,+\, \eta_{\rm t}{\rm Rm}\langle \bar{J}{\cdot}\bar{B}/B_{\rm eq}^2\rangle \,+\, {\rm fluxes}}{1 \,+\, {\rm Rm}\;\langle \bar{B}^2\rangle/B_{\rm eq}^2}$$

  - catastrophic quenching $(\bar{J} = 0$, no fluxes$)$:

$$\alpha \;=\; \frac{\alpha_{\rm K}}{1 \,+\, {\rm Rm}\;\langle \bar{B}^2\rangle/B_{\rm eq}^2}$$

  - fully helical large-scale field $(\langle\,\bar{J}\cdot\bar{B}\,\rangle = k_{\rm m}\bar{B}^2)$:

$$\alpha \;=\; \frac{\alpha_{\rm K} \,+\, \eta_{\rm t}\;k_{\rm m}\;{\rm Rm}\langle\bar{B}^2\rangle/B_{\rm eq}^2}{1 \,+\, {\rm Rm}\;\langle \bar{B}^2\rangle/B_{\rm eq}^2} \rightarrow k_{\rm m}\,\eta_{\rm t}$$

Compared to the kinematic value $\alpha_{\rm K} \simeq k_{\rm f}\,\eta_{\rm t}$,
α is quenched by the scale-separation ratio $k_{\rm m}/k_{\rm f}$.

a lingering catastrophe

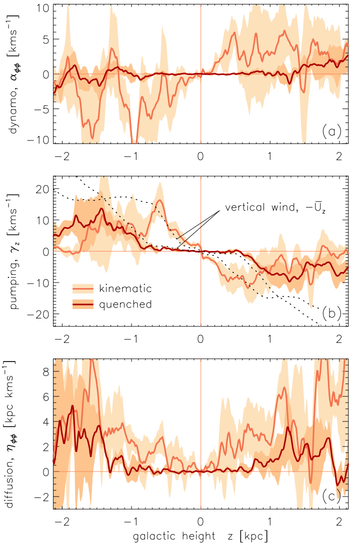

- Quenching scenarios:
  - (a) classic: flow quenching due to Lorentz force
  - (b) catastrophic: helicity conservation inhibits growth
  - (c) similar to scenario (b) but alleviated by small-scale helicity removal
- Test possible realisations:
  - quenching sets-in . . .
    (a) . . . at $B \simeq B_{\rm eq}$
    (b) . . . at $B \simeq B_{\rm eq}/{\rm Rm}$
    (c) . . . at $B \simeq B_{\rm eq}\, l_0/L_0$
- Suppression of wind: (c) $\rightarrow$ (b)

extracting quenching functions

- quenching quadratic in $\beta \equiv \bar{B}/B_{\rm eq}$
- magnetic Reynolds number, $\mathrm{Rm} \equiv u_{\rm rms}(k_{\rm f}\,\eta)^{-1} \simeq 75\text{–}125$
- scale separation ratio, $l_0/L_0 \simeq 0.1\,\mathrm{kpc}/1\,\mathrm{kpc} = 10$

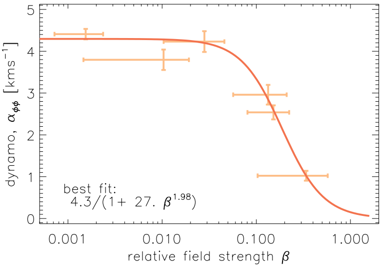

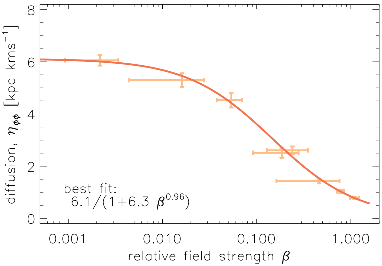

Gressel, Bendre & Elstner (2013), MNRAS 429, 967

the disc model

- Based on flaring HI disc
  Kalberla & Dedes (2008)
  - expon. + power-law density profile
  - NFW-type DM halo + stellar disc / bulge
  - → self-consistent rotation curve

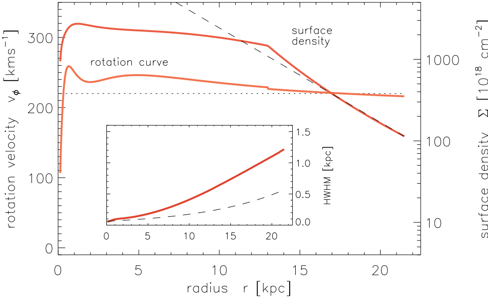

- Goal: perform fully-dynamical MHD + MFD simulations
  - momentum equation with turbulent viscosity
  - will capture Parker / Tayler / MRI on long wavelengths

emerging dynamo mode

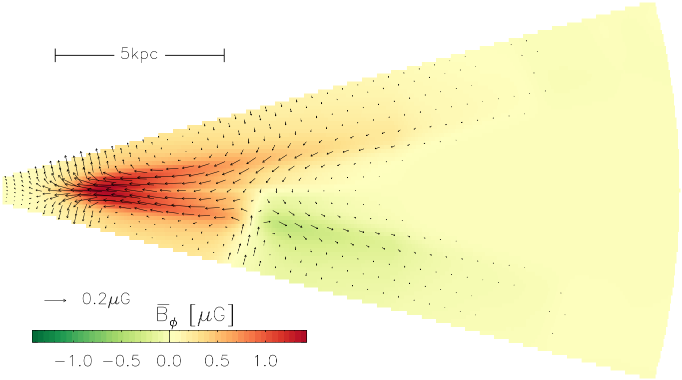

- initial NVF leads to transient A0, → S0 mode
- S0+A0 produces one-sided vertical field Mao, Gaensler et al. (2010)

model overview

Table 2. Simulation parameters and results.

model	dim	MF	NS	halo	M_{gas} [$10^{10}M_\odot$]	seed	parity	p_{in} [°]	p_{out} [°]	τ_e [Gyr]	$\lvert\overline{\mathbf{B}}_{sat}\rvert$ [μG]	comments
X1s-0.5	2D	•	○	○	0.57	WN	S0/A0	-31.2	-4.7	0.374	1.44	see Fig. 3
X1s	2D	•	○	○	1.14	WN	S0[a]	-28.7	-4.6	0.503	3.75	see Figs. 4,5
X1s-1.5	2D	•	○	○	1.70	WN	S0[a]	-32.7	-4.6	0.547	6.34	
X1s-2.0	2D	•	○	○	2.27	WN	S0	-35.8	-4.3	0.593	9.07	
X2s-halo	2D	•	○	•	1.14	WN	S0[a]	-25.2	-4.8	0.358	4.05	
X3s-VF	2D	•	○	○	1.14	NVF	A0→S0	-28.9	-4.5	0.539	3.75	
N1s/d-HF	3D	•	○	○	1.14	NHF	S0	-28.7	-3.2	–	3.75	
	3D	•	•	○	1.14		S0	-17.7	-2.6	–	2.52	
N1s/d-VF	3D	•	○	○	1.14	NVF, B_ϕ	S0	-29.0	-6.1	0.409	3.75	
	3D	•	•	○	1.14		S0	-17.8	-2.7	0.407	2.65	see Fig. 8
N2d	3D	○[b]	•	○	1.14	HF+VF	A0	-5.3	-1.6	–	0.82[c]	see Fig. 6
N2d-MRI	3D	○	•	○	1.14	HF+VF	A0	-6.0	-0.5	–	4.25	see Fig. 7

[a] sub-dominant A0 outside $R \simeq 10$ kpc, [b] includes η_t, and ν_t, [c] obtained outside $R \simeq 15$ kpc.

All 2D runs are axisymmetric; mean-field (MF) effects include the ones described in Sect. 2.2; runs including 'NS' evolve the Navier-Stokes equation. The 'halo' dynamo is shown as a dashed line in Fig. 2. The column labelled M_{gas} gives the normalisation for the disc mass. For seed fields we use white noise (WN), net-vertical field (NVF), net-horizontal field (NHF). Pitch angles are given for the inner disc (peak value) and for the outer disc (average for $R > 10$ kpc) separately. Growth rates are for the magnetic field $|\overline{\mathbf{B}}|$, during an interval for which exponential growth can be identified.

Gressel, Elstner & Ziegler (2013) A&A 560, 93

radial pitch angle

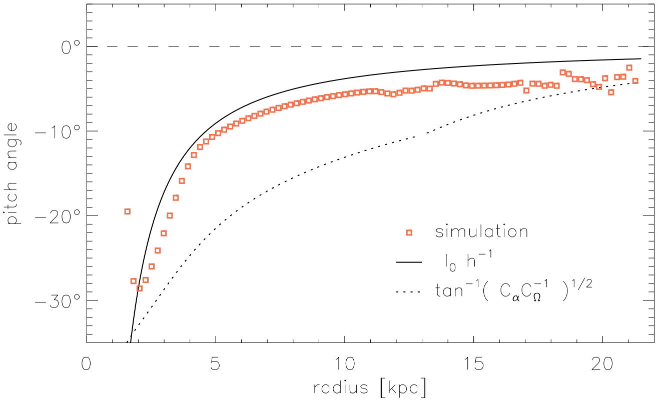

- radial fall-off in pitch angle (agrees with observations)
- → explained conveniently by flaring disc Fletcher (2010)

saturated field profile

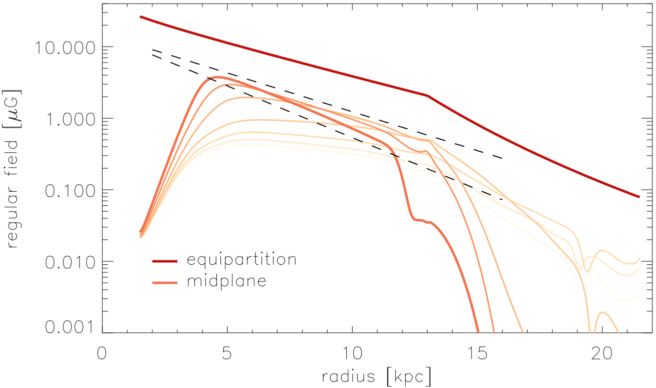

- radial scale length $\sim 4\,\mathrm{kpc}$ for saturated $\overline{\mathbf{B}}$
- outer disc essentially unmagnetised

MHD w/o mean-field dynamo

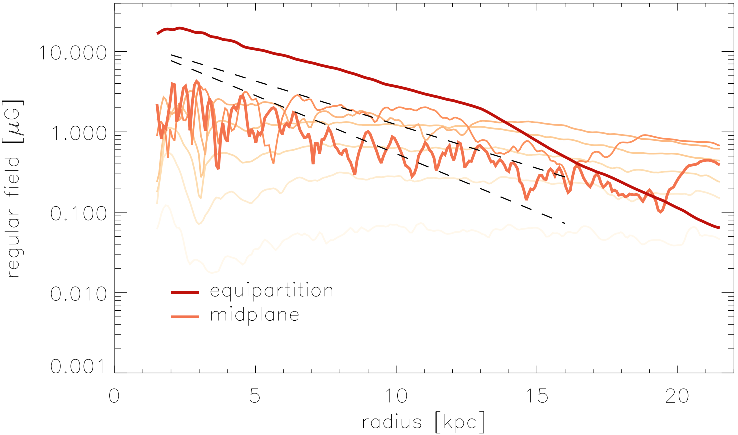

MRI-only simulation   MRI with dissipation from SNe

MHD w/o mean-field dynamo

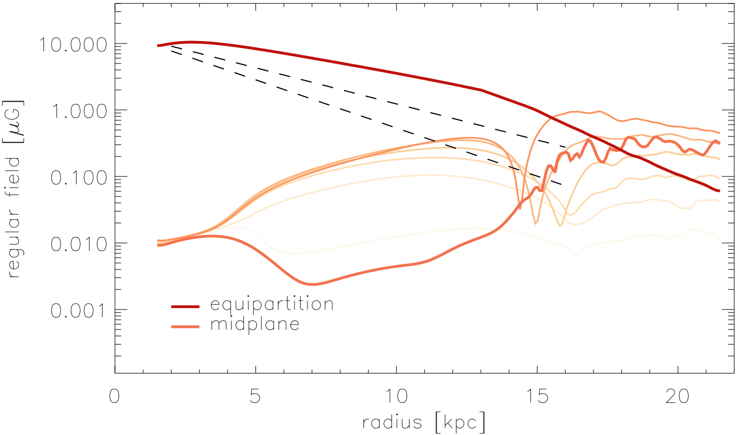

MRI-only simulation MRI with dissipation from SNe

combined MHD / mean-field dynamo

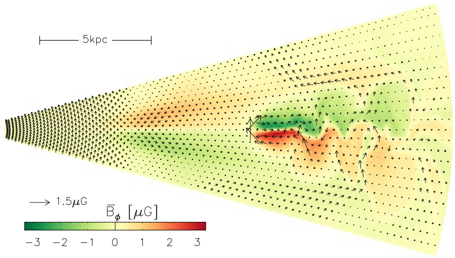

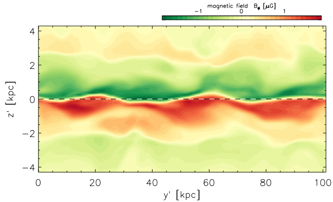

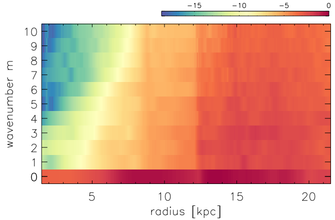

- Parker modes & MRI in outer disc
  $\rightarrow$ pronounced loop structures
- undulating mode with $m = 3$
- radial scale length $\sim 10\,\mathrm{kpc}$
- inner disc dominated by $m = 0$

Do magnetic fields influence rotation in galaxies?

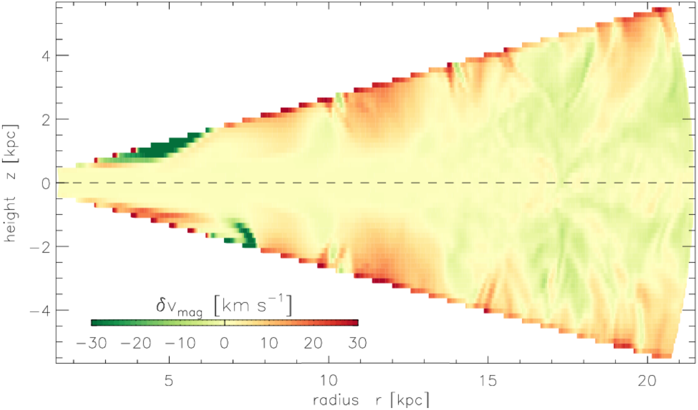

prediction from Lorentz force   actual result from simulation

Elstner, Beck & Gressel (2014) A&A 568, A104

Do magnetic fields influence rotation in galaxies?

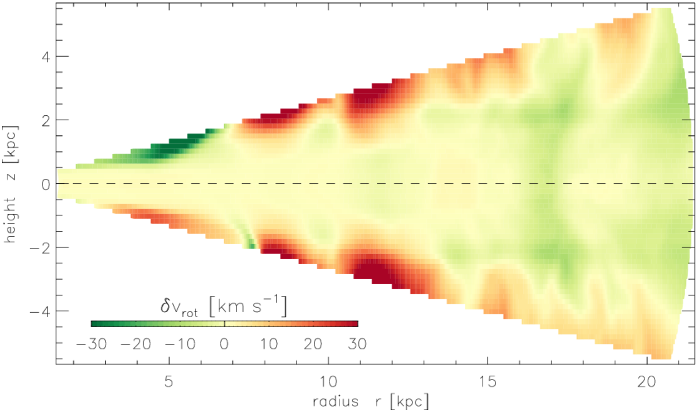

prediction from Lorentz force actual result from simulation

Elstner, Beck & Gressel (2014) A&A 568, A104

synthetic polarisation maps

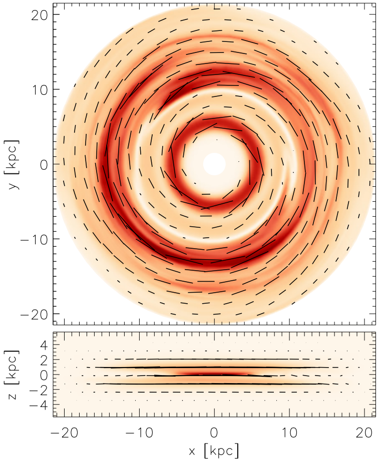

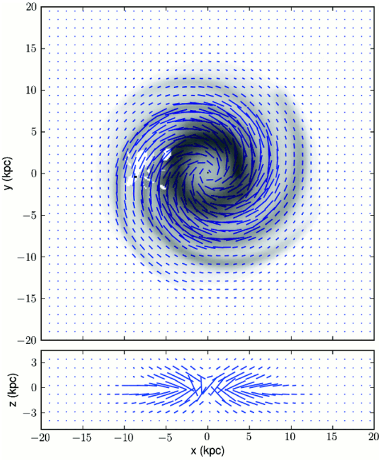

Jansson & Farrar (2012)

summary of results

- Measuring dynamo coefficients
  - 1D mean-field model matches simulations
  - $\rightarrow$ quantitative scaling relations for sub-grid physics
- Non-linear saturation
  - quenching functions obtained
  - indications for the presence of helicity constraints
  - suppression of wind threatens saturation level
- Global mean-field models
  - first fully quantitative global dynamo models
  - dynamic momentum equation $\rightarrow$ MRI / Parker / Tayler
  - parametrisation of small-scale effects is essential

summary of results

- Measuring dynamo coefficients
  - 1D mean-field model matches simulations
  - $\rightarrow$ quantitative scaling relations for sub-grid physics
- Non-linear saturation
  - quenching functions obtained
  - indications for the presence of helicity constraints
  - suppression of wind threatens saturation level
- Global mean-field models
  - first fully quantitative global dynamo models
  - dynamic momentum equation $\rightarrow$ MRI / Parker / Tayler
  - parametrisation of small-scale effects is essential

summary of results

- Measuring dynamo coefficients
  - 1D mean-field model matches simulations
  - $\rightarrow$ quantitative scaling relations for sub-grid physics
- Non-linear saturation
  - quenching functions obtained
  - indications for the presence of helicity constraints
  - suppression of wind threatens saturation level
- Global mean-field models
  - first fully quantitative global dynamo models
  - dynamic momentum equation $\rightarrow$ MRI / Parker / Tayler
  - parametrisation of small-scale effects is essential